Resonance Raman Spectroscopic Characterization of α-Hydroxyheme and Verdoheme Complexes of Heme Oxygenase†

Satoshi Takahashi,‡,§ Kathryn Mansfield Matera,||,⊥ Hiroshi Fujii,▽ Hong Zhou,# Kazunobu Ishikawa,# Tadashi Yoshida,# Masao Ikeda-Saito,*,|| and Denis L. Rousseau@

Institute for Physical and Chemical Research (RIKEN), Wako 351-01, Japan, Department of Physiology and Biophysics, Case Western Reserve University School of Medicine, Cleveland, Ohio 44106-4970, Institute for Life Support Technology, Yamagata Technopolis Foundation, Yamagata 990, Japan, Department of Biochemistry, Yamagata University School of Medicine, Yamagata 990-23, Japan, and Department of Physiology and Biophysics, Albert Einstein College of Medicine, Bronx, New York 10461

Received September 18, 1996; Revised Manuscript Received November 25, 1996⊗

ABSTRACT: Heme oxygenase (HO) is the microsomal enzyme that catalyzes the oxidative degradation of protoheme (iron protoporphyrin IX) and the generation of carbon monoxide. The enzyme converts protoheme into biliverdin through two known heme derivatives, α-hydroxyheme and verdoheme. To gain insight into the degradation mechanisms of the two intermediates, the resonance Raman spectra were observed for α-hydroxyheme and verdoheme complexes of HO and compared with those of apomyoglobin (apo-Mb) complexes. The ferrous α-hydroxyheme complexed with both HO and apo-Mb shows a resonance Raman spectral pattern similar to that of the protoheme complexes. On the contrary, the ferric α-hydroxyheme and ferrous verdoheme complexes of HO and apo-Mb show atypical Raman patterns, which are interpreted as the result of the symmetry lowering of the porphyrin-conjugated π-electron system. The comparison of the resonance Raman spectra of the verdoheme complexed with HO and apo-Mb with those of the five- and six-coordinate model complexes of verdoheme shows that the ferrous forms of the verdoheme−protein complexes are six-coordinate. The Fe−CO and Fe−CN stretching frequencies of ferrous verdoheme compounds are distinct from those of ferrous heme compounds. It is inferred that the positive charge of the verdoheme ring possesses some of the charge density on the iron atom, causing unique characteristics of the iron ligand stretching vibrations and altered ligand binding properties.

Heme oxygenase (HO), an amphipathic microsomal protein, catalyzes the regiospecific ring opening of heme (iron protoporphyrin IX) to biliverdin by using molecular oxygen (O_2) and electrons donated by cytochrome P450 reductase (Tenhunen *et al.*, 1969; Kikuchi & Yoshida, 1983; Maines, 1988). This rate-limiting process of the heme catabolism is responsible for the generation of carbon monoxide (CO), a putative biological messenger molecule (Verma *et al.*, 1993; Zhuo *et al.*, 1993; Stevens *et al.*, 1993; Suematsu *et al.*, 1995). The enzyme binds 1 equiv of heme, thus forming a heme−protein complex in which the heme iron is coordinated to a histidine in a manner similar to that seen in myoglobin (Mb) and hemoglobin (Yoshida & Kikuchi, 1978a). The distal site of the heme is then used to coordinate and activate O_2 which leads to the regiospecific hydroxylation of the α-meso carbon of the heme (Yoshida *et al.*, 1980a; Takahashi *et al.*, 1995). This is the first of three cycles of oxygenation reactions conducted by HO. At the second oxygenation step, the enzyme converts the α-hydroxyheme to verdoheme with the release of CO (Yoshida *et al.*, 1981, 1982). In the final oxygenation step, the verdoheme is converted to a biliverdin−iron complex, which is released from the enzyme as ferrous iron and biliverdin to conclude the turnover (Scheme 1) (Yoshida & Kikuchi, 1978b). It is notable that a single enzyme can catalyze such diverse reactions, each of which oxygenates the heme catabolic intermediates having different electronic and coordination characteristics as well as reactivities with oxygen.

Using recombinant HO preparations (Ishikawa *et al.*, 1991; Ito-Maki *et al.*, 1995), many of the enzyme's structural properties and their functional relevance have been investigated. Recent studies have shown that a neutral form of the imidazole ring of His-25 is the axial ligand in the heme−enzyme (isoform-1) complex (Takahashi *et al.*, 1994a,b; Sun *et al.*, 1994; Ito-Maki *et al.*, 1995). While this coordination structure is atypical for oxygenases (Dawson, 1988; Poulos, 1988), the neutral ligand coordination is hypothesized to stabilize a ferric-hydroperoxide intermediate, Fe(III)-OOH, as the putative oxygen-activated form of the enzyme in the first oxygenation cycle (Noguchi *et al.*, 1983; Wilks & Ortiz de Montellano, 1993). The enzyme directs the hydroper-

† This work was supported by Research Grants GM51588 (M.I.-S.) and GM48714 (D.L.R.) from the National Institutes of Health and by Grants-in-Aid for Scientific Research 08249101, 08044240, and 08680675 (T.Y.) from the Ministry of Education, Science, Sports and Culture, Japan. S.T. was supported by the Special Postdoctoral Researchers Program at RIKEN.

* To whom correspondences should be addressed: Dr. Masao Ikeda-Saito, Department of Physiology and Biophysics, Case Western Reserve University School of Medicine, Cleveland, OH 44106-4970. Phone: (216) 368-3178. Fax: (216) 368-3952. E-mail: mis2@po.cwru.edu.

‡ RIKEN.

§ Present address: Department of Molecular Engineering, Graduate School of Engineering, Kyoto University, Kyoto 606, Japan.

|| Case Western Reserve University School of Medicine.

⊥ Present address: Department of Chemistry, Baldwin-Wallace College, Berea, Ohio 44107.

▽ Yamagata Technopolis Foundation.

Yamagata University School of Medicine.

@ Albert Einstein College of Medicine.

⊗ Abstract published in *Advance ACS Abstracts,* January 1, 1997.

S0006-2960(96)02361-6 CCC: $14.00

Scheme 1: Intermediates in the Reaction of the Heme-Oxygenase-Catalyzed Conversion of Iron Protoporphyrin IX to the Biliverdin−Iron Complex

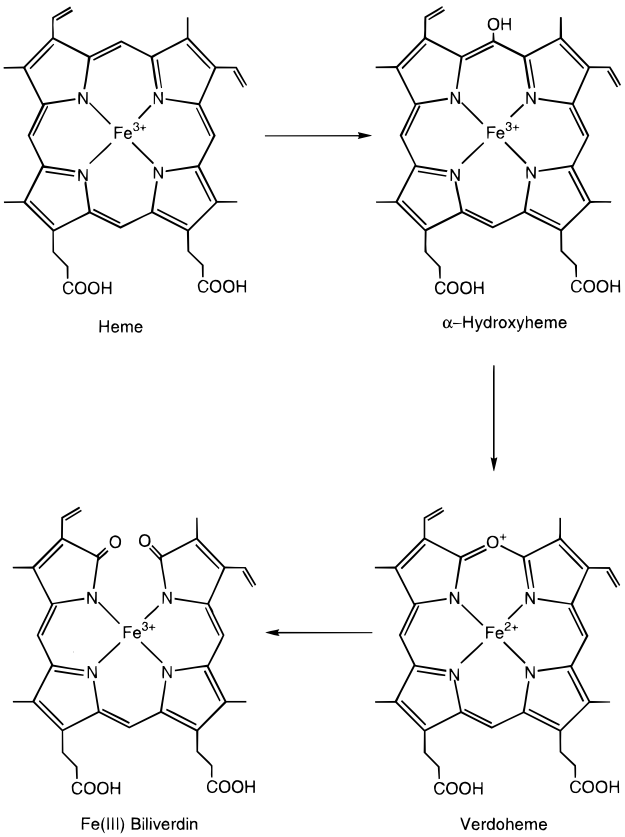

oxide toward the α-meso carbon through electronic and steric interactions, thus causing regiospecific attack in the first oxygenation step (Hernandez *et al.*, 1994; Takahashi *et al.*, 1995). Two reaction mechanisms are proposed for the second oxygenation cycle, during which α-hydroxyheme is converted to verdoheme. The first mechanism is the direct attack of O_2 at the ring carbon of ferric α-hydroxyheme followed by one-electron reduction (Sano *et al.*, 1986; Mansfield Matera *et al.*, 1996). Model compound studies showed that the ionizable hydroxyl group has a resonance form which includes radical character on the macrocycle that behaves as a target for the O_2 attack (Morishima *et al.*, 1986, 1995; Fujii, 1990). In the second proposed mechanism, the O_2 attacks α-hydroxyheme after its reduction to the ferrous state (Chang *et al.*, 1994; Mansfield Matera *et al.*, 1996). Although the necessity of both O_2 and reducing equivalent(s) exists for the conversion of verdoheme to biliverdin (Brown & King, 1976; Saito & Itano, 1982; Yoshida & Noguchi, 1984), mechanistic studies using the verdoheme complex of HO have not been undertaken except for the pioneering efforts by Yoshida and his collaborators (Yoshida *et al.*, 1980b; Noguchi *et al.*, 1981; Yoshida & Noguchi, 1984).

The variety of reaction mechanisms exhibited by HO in these three oxidative steps should be a reflection of the diverse characteristics of the enzyme's heme degradation intermediates. However, knowledge of the electronic and ligand binding properties of α-hydroxyheme and verdoheme is insufficient, thereby limiting the understanding of their degradative mechanisms. We have therefore obtained and analyzed resonance Raman spectra of α-hydroxyheme and verdoheme complexed with HO and apo-Mb as well as examined verdoheme model complexes. The observed spectral patterns and the frequencies of the iron−ligand stretching modes are unique among those observed for the protoheme proteins. However, the charge neutrality principle can explain most of the observations qualitatively. Contrary to the previous premise (Sano *et al.*, 1986), we conclude that the ferrous form of verdoheme complexed with HO and apo-Mb is very likely to be six-coordinate. These results are essential to understanding the reaction mechanisms of the heme degradation by HO.

EXPERIMENTAL PROCEDURES

Verdoheme (protoverdoheme IXα) was synthesized as described by Saito and Itano (1986). The α-hydroxyheme (α-hydroxyprotoheme) samples were made by hydrolyzing α-(benzoyloxy)protohemin as described in Mansfield Matera *et al.* (1996).

The enzymatically active water soluble fragment of the rat HO isoform-1, which lacks the C-terminal membrane-bound segment with S262A and S263L mutations, was expressed and purified as described previously (Ito-Maki *et al.*, 1995). The ferric α-hydroxyheme- and ferrous verdoheme−HO complexes were prepared as described by Mansfield Matera *et al.* (1996) and Fujii (1990), respectively. The ferric α-hydroxyheme- and ferrous verdoheme−Mb complexes were reconstituted by the same procedures using the apo-Mb prepared from horse Mb by the procedure described by Teale (1959). All samples were reconstituted inside a nitrogen glovebox and sealed in Raman cells. The concentrations of the complexes used for Raman measurements were typically 20 μM.

The ferrous verdoheme compounds with pyridine, imidazole, and 2-methylimidazole as axial ligand(s) were made by dissolving verdoheme solid into a 50% solution of pyridine, a 10 M solution of imidazole, and a 50 mM solution of 2-methylimidazole with 0.05% SDS, respectively. All samples were in 50 mM phosphate buffer, at pH 7. The ferric six-coordinate and ferrous five-coordinate verdoheme complexes were prepared by the method described by Balch *et al.* (1993) except for the substitution of protoverdoheme IXα as the starting material. In brief, verdoheme was dissolved in a 2% solution (v/v) of hydrochloric acid in methanol. The solvent was immediately removed under vacuum, and the resultant solid was used as the ferric complex. The dichloromethane solution of the ferric complex was stirred with solid dithionite under anaerobic conditions. The reduced sample was used as the ferrous five-coordinate complex. The formation of each species was confirmed by optical absorption spectra (Figure 6) using the spectral data from Balch *et al.* (1993) as the standard.

Optical absorption spectra were recorded on an SLM-Aminco or Hewlett-Packard spectrophotometer. The 406.7 and 413.1 nm lines of a krypton ion laser (Spectra Physics, Mountain View, CA) and the 441.6 nm line of a helium−cadmium laser (Liconics, Santa Clara, CA) were used for Raman excitation. The powers of the excitation lasers were set at 5−10 mW at the sample point unless otherwise stated. The sample cell was rotated at ca. 1000 rpm. The Raman scattered light was dispersed by a single polychrometer (Spex, Metuchen, NJ) and detected by a liquid nitrogen-cooled CCD camera (Princeton Instruments, Princeton, NJ). The spectral slit width was set to about 5 cm^{-1}, and the Raman shifts were calibrated by using indene as a frequency

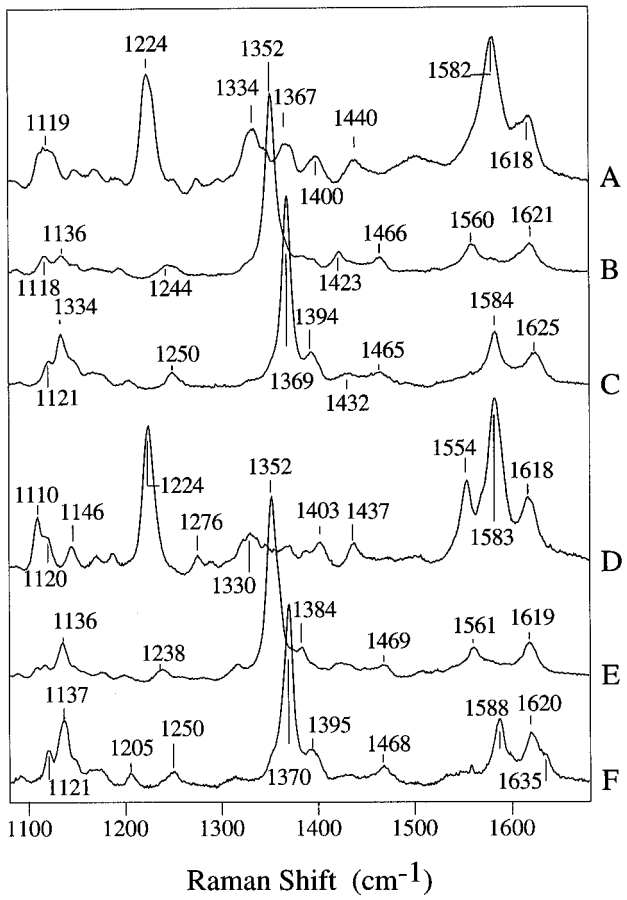

FIGURE 1: High-frequency resonance Raman spectra of α-hydroxyheme complexed with HO and apo-Mb: α-hydroxyheme−HO complex in the ferric (trace A), ferrous (trace B), and ferrous-CO-bound (trace C) forms and α-Hydroxyheme−Mb complex in the ferric (trace D), ferrous (trace E), and ferrous-CO-bound (trace F) forms. The ferric spectra (traces A and D) were recorded using 406.7 nm excitation, while other forms were recorded using 413.1 nm excitation. The Raman lines associated with contaminated verdoheme−HO complex were subtracted from trace A.

standard. Noise in the spectra caused by cosmic rays was removed by a standard software package (CSMA, Princeton Instruments).

RESULTS

α-*Hydroxyheme−HO and −Mb Complexes.* The optical absorption spectra of the α-hydroxyheme complexes of HO are reported elsewhere (Mansfield Matera *et al.*, 1996). Figure 1 depicts the resonance Raman spectra in the high-frequency region (1100−1700 cm^{-1}) of the α-hydroxyheme complexed with both HO and apo-Mb in ferric, ferrous, and ferrous-CO-bound forms. In general, the observed spectral patterns for ferrous and ferrous-CO compounds are similar to those observed for protoheme complexes of HO. For example, a strong ν_4 line at 1352 cm^{-1} and weaker ν_2 and ν_3 lines at 1560 and 1466 cm^{-1}, respectively, observed for the ferrous form of the HO complex (trace B) all have frequencies slightly lower (within 4 cm^{-1}) than the corresponding modes observed for the protoheme complexes of HO (Takahashi *et al.*, 1994b). The CO derivative of the HO complex (trace C) and ferrous (trace E) and ferrous-CO derivative (trace F) of the Mb complex all show this tendency. Unlike the ferrous species, the ferric species show unique Raman spectral patterns for both HO (trace A) and Mb (trace D) complexes (Mansfield Matera *et al.*, 1996).

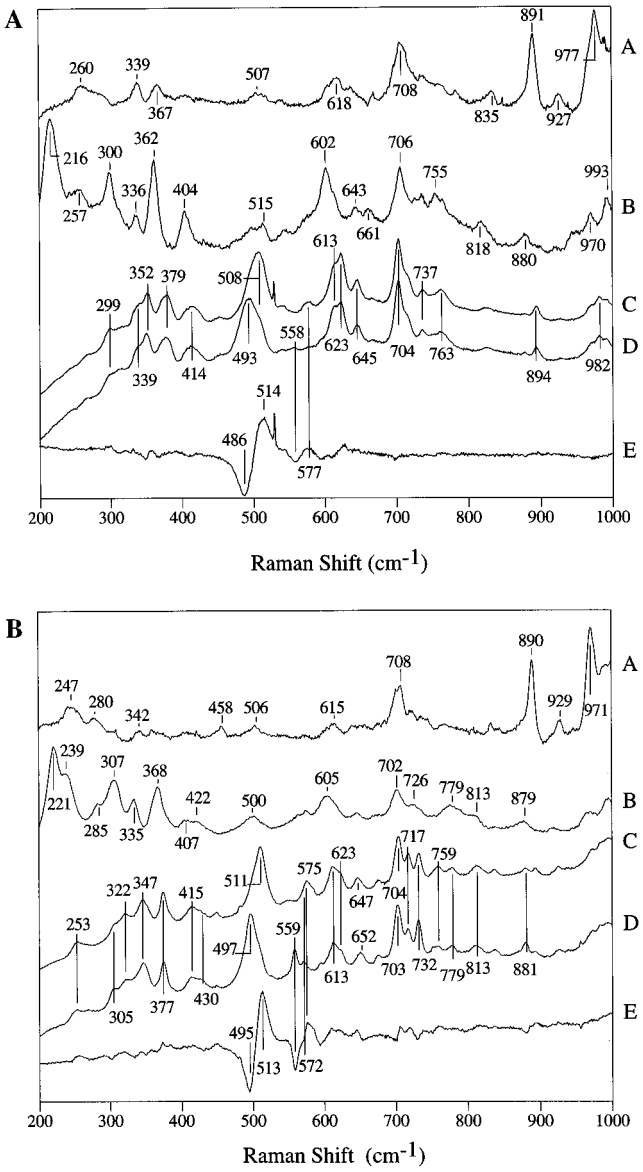

FIGURE 2: Low-frequency resonance Raman spectra of α-hydroxyheme complexed with HO (panel A) and apo-Mb (panel B). (panel A) Trace A, α-hydroxyheme−HO complex in the ferric form excited at 406.7 nm; trace B, the ferrous complex excited at 441.6 nm; traces C and D; the ferrous-$^{12}C^{16}O$-bound (trace C) and -$^{13}C^{18}O$-bound (trace D) forms excited at 413.1 nm; and trace E, difference Raman spectrum between traces C and D. (panel B) Trace A, α-hydroxyheme−Mb complex in the ferric form excited at 406.7 nm; trace B, the ferrous complex excited at 441.6 nm; traces C and D, the ferrous-$^{12}C^{16}O$-bound (trace C) and -$^{13}C^{18}O$-bound (trace D) forms excited at 413.1 nm; and trace E, difference Raman spectrum between traces C and D.

Two major differences between the ferric α-hydroxyheme and the analogous ferric protoheme include the following. (1) The strong ν_4 mode cannot be observed, but the two Raman lines at around 1220 and 1580 cm^{-1} are enhanced. (2) The majority of observed lines in the ferric state are broader than those in both ferrous and ferrous-CO-bound forms.

Panels A and B of Figure 2 demonstrate the low-frequency region of the resonance Raman spectra obtained for HO and apo-Mb complexed with α-hydroxyheme, respectively. In all the redox states for the α-hydroxyheme complexes that were examined (ferric, ferrous, and ferrous-CO-bound forms), the strong ν_7 line near 670 cm^{-1} that typically appears for protoheme complexes is not seen. The line at 602 cm^{-1} for

the ferrous HO complex (Figure 2A, trace B) shows a 3 cm^{-1} shift to low frequency upon D_2O substitution (Mansfield Matera *et al.*, 1996). The line at 623 cm^{-1} for the CO-bound ferrous complex (Figure 2A, trace C) also shows a similar deuterium shift. Thus, these lines can probably be assigned as ν_7. Since the ν_7 involves the largest movement of the meso carbons among the totally symmetric modes (Abe *et al.*, 1978; Spiro & Li, 1988), the hydroxyl substitution on the α-meso carbon likely induces its shift to low frequency. The Fe−His stretching vibrations (Kitagawa, 1988) are also observed in the low-frequency region at 216 and 221 cm^{-1} for the ferrous α-hydroxyheme complexes of HO (Figure 2A, trace B) and Mb (Figure 2B, trace B), respectively. These frequencies coincide with the Fe−His modes of the protoheme complex of both HO and Mb and confirms their assignments (Takahashi *et al.*, 1994b). Furthermore, the spectral pattern observed between 200 and 400 cm^{-1} for the ferrous and ferrous-CO-bound α-hydroxyheme complexes are very similar to those obtained for the protoheme complexes. Since the low-frequency modes mainly reflect the out of plane deformation of the heme and the conformation of the peripheral substituents (Spiro & Li, 1988; Hu & Spiro, 1993), the interactions between the ferrous α-hydroxyheme and the protein matrix appear to be similar to those of the protoheme complex. Traces C and D of Figure 2A show the $^{12}C^{16}O$ and $^{13}C^{18}O$ derivatives of α-hydroxyheme−HO complex, respectively. The two modes associated with the Fe−CO unit, Fe−CO stretching (508 cm^{-1}) and Fe−C−O bending (577 cm^{-1}) lines, are apparent from the isotopic difference spectrum shown as trace E. Corresponding spectra for the Mb complex are shown in Figure 2B. Carbonyl (C═O) stretching lines are also observed in the 1900−2000 cm^{-1} region of the Raman spectra and identified at 1963 and 1945 cm^{-1} for the HO and Mb complexes, respectively, using isotopic shifts (data not shown). These observed frequencies of the ferrous α-hydroxyheme-enzyme complexes coincide well with those of the corresponding protoheme−CO complexes (Takahashi *et al.*, 1994b).

Verodoheme−HO and −Mb Complexes. Figure 3 shows the optical absorption spectra of verdoheme −HO complexes. Traces A−C represent the ferrous, ferrous-CO, and cyanide (CN^-)-bound forms of the HO complexes, respectively. The corresponding absorption spectra for the Mb complexes are consistent with the reported spectra (Sano *et al.*, 1986; Fujii, 1990). Yoshida and Noguchi (1984) trapped a catalytic intermediate of HO that shows 688, 638, and 690 nm absorption peaks for ferrous, CO, and CN^--bound forms, respectively, and assigned the intermediate as the verdoheme−HO complex. The present HO complex has peaks at 685, 637, and 691 nm, thus confirming their assignments. The resonance Raman spectra of the verdoheme−HO and −Mb complexes in the high-frequency region are presented in Figure 4. The spectra show an atypical pattern compared with the protoheme complexes but retain similarity to that of the ferric α-hydroxyheme complexes. In general, two strong lines near 1250 and 1610 cm^{-1} exist, with several weaker lines between them.

The resonance Raman spectra of the ferrous verdoheme−protein complexes (Figure 4, traces A and D for HO and Mb complexes, respectively) are almost identical with those of the CN^--bound complexes (Figure 4, traces C and F). The optical absorption spectra also demonstrate the similarity of the ferrous (Figure 3, trace A) and CN^--bound (Figure 3, trace C) species. On the contrary, the CO-bound complexes show distinct Raman (Figure 4, traces B and E) and optical (Figure 3, trace B) spectroscopic patterns. We could not observe any change in the ferrous Raman spectra by changing excitation laser power between 1 and 30 mW. The CO ligand of the CO-bound complexes is extremely photolabile, as indicated by the low excitation power necessary to measure the CO-bound enzyme complex (∼500 μW). The spectra for isotopically labeled cyanide ($^{13}C^{15}N^-$)- and carbon monoxide ($^{13}C^{18}O$)-bound forms do not show any differences from those of the respective natural abundance complexes in the high-frequency region (data not shown).

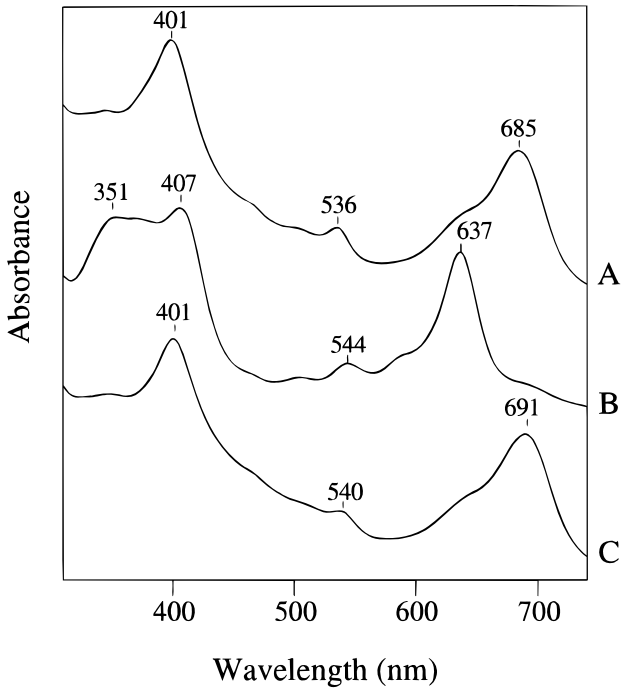

FIGURE 3: Optical absorption spectra of verdoheme−HO complex in the ferrous (trace A), ferrous-CO-bound (trace B), and ferrous-CN^--bound (trace C) forms. The ordinate scales are arbitrary.

The low-frequency Raman spectra of the verdoheme−HO and −apo-Mb complexes are displayed in panels A and B of Figure 5, respectively. We can observe intense and moderate lines at around 660 and 340 cm^{-1}, respectively, which can be assigned to the ν_7 and ν_8 modes, respectively. The $^{12}C^{16}O$ minus $^{13}C^{18}O$ difference spectra (traces D of Figure 5A,B) show the presence of Fe−CO stretching lines at 474 and 468 cm^{-1} and Fe−C−O bending lines at 564 and 565 cm^{-1} for the HO and Mb complexes, respectively. The $^{12}C^{14}N$ minus $^{13}C^{15}N$ difference spectra (traces G of Figure 5A,B) show the Fe−CN stretching modes at 474 and 473 cm^{-1} for the HO and Mb complexes, respectively. The Fe−C−N bending mode for the apoMb complex is observed at 313 cm^{-1}. The Fe−CN stretching lines are split as indicated by the presence of two negative peaks. No isotopically sensitive lines were detected between 1700 and 2400 cm^{-1} for either CO- or CN^-- bound forms (data not shown). The ferrous spectra (traces A) do not show any Raman lines assignable as the Fe−His mode. The absence of the Fe−His line and the spectral similarities observed between the ferrous and CN^-- bound species suggest that the ferrous complexes are six-coordinate. In the case of Mb, the distal histidine (His-64) is the likely candidate for the sixth ligand; however, this possibility has been eliminated as a mutant apo-Mb with the distal His replaced by Ile

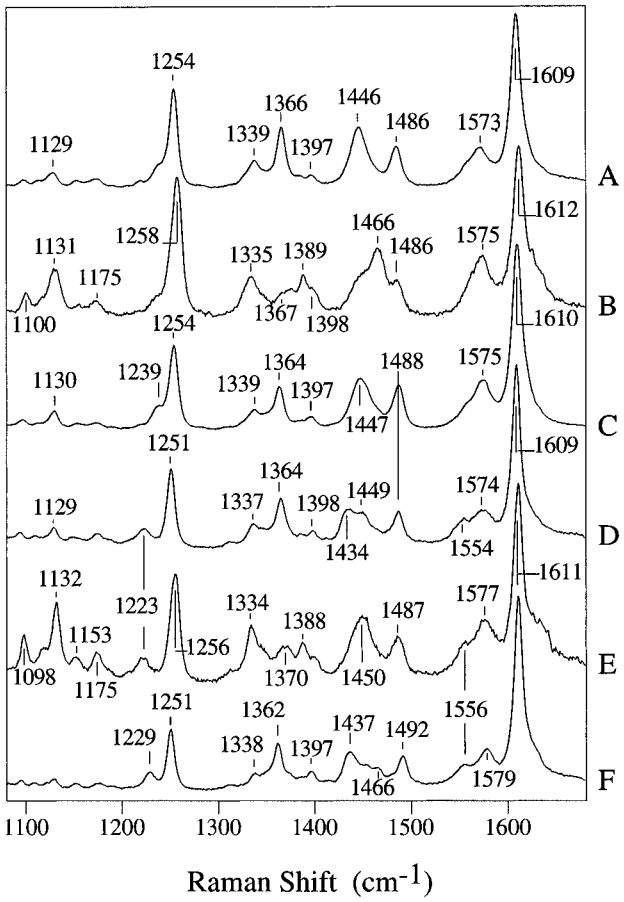

FIGURE 4: High-frequency resonance Raman spectra of verdoheme complexed with HO and apo-Mb: verdoheme−HO complex in the ferrous (trace A), ferrous-CO-bound (trace B), and ferrous-CN^--bound (trace C) forms and verdoheme−Mb complex in the ferrous (trace D), ferrous-CO-bound (trace E), and ferrous-CN^--bound (trace F) forms. All spectra were obtained using 406.7 nm excitation with ca. 5 mW of laser power except for CO complexes (B and E) which were obtained with ca. 0.5 mW of power.

reconstituted with verdoheme has an optical absorption spectrum identical with that of wild type complex (data not shown). Other likely ligands at the sixth coordination site include water and hydroxide. No D_2O shifts were observed, however, in the Raman spectrum of the verdoheme−HO complex (data not shown).

Model Verdoheme−HO Complexes. The above results suggest that the deoxy verdoheme is six-coordinate, although the atypical Raman spectra precludes us from determining the coordination structure. In an effort to resolve the coordination number question, we analyzed Raman spectra of verdoheme model complexes with known coordination and redox states to establish the correlation between Raman spectra and coordination states. Figures 6 and 7 show the optical absorption and resonance Raman spectra, respectively, of six-coordinate ferric, five-coordinate ferrous, and six-coordinate CO-bound ferrous forms of verdoheme (Balch *et al.*, 1993). The spectra of bis-imidazole-coordinated ferrous verdoheme are also presented. The ferric complex has Raman lines at 1599 and 1241 cm^{-1} (Figure 7, trace A), whereas the ferrous five-coordinate species exhibits lines at 1596 and 1243 cm^{-1} (trace B). The addition of CO to the ferrous five-coordinate complex causes the shifts of the two intense lines to higher frequencies (1613 and 1254 cm^{-1}, trace C) that are similar to those of the CO-bound verdoheme complex of HO (Figure 4, trace B). In addition, the bis-

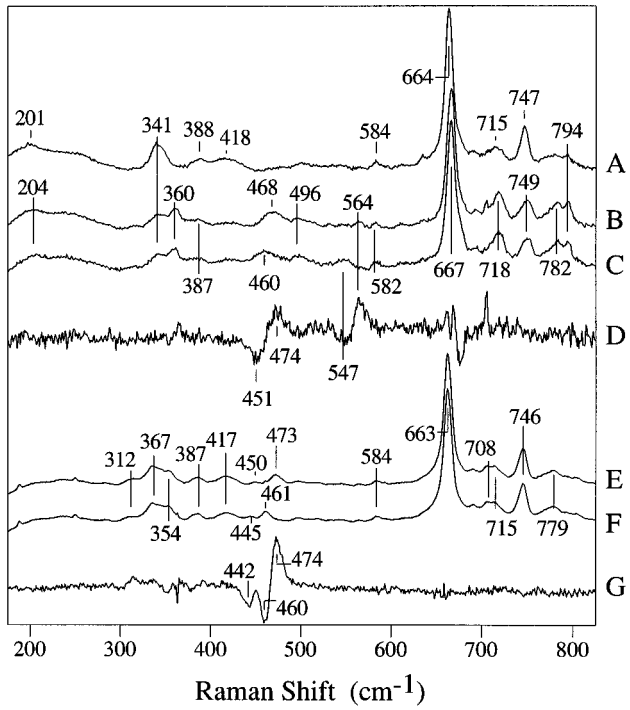

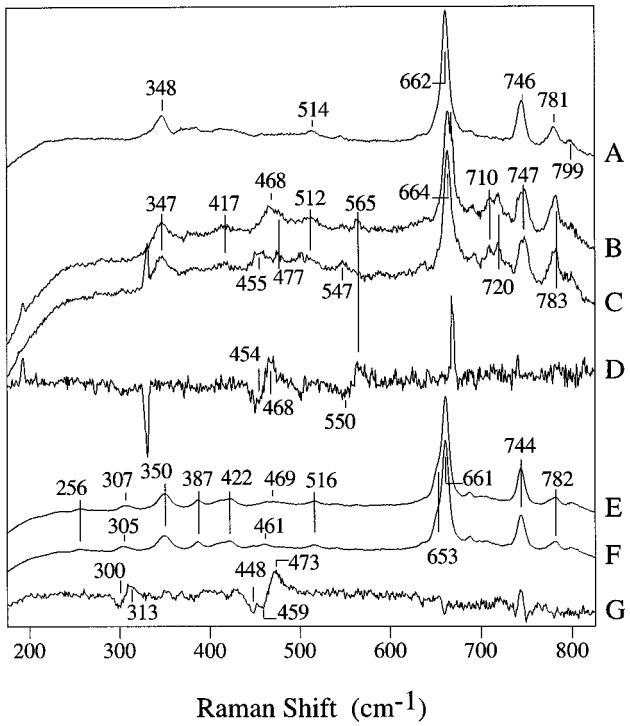

FIGURE 5: Low-frequency resonance Raman spectra of verdoheme complexed with HO (panel A) and apoMb (panel B). (panel A) Verdoheme−HO complex in the ferrous (trace A), ferrous-$^{12}C^{16}O$-bound (trace B), ferrous-$^{13}C^{18}O$-bound (trace C), ferrous-$^{12}C^{14}N$-bound (trace E) and ferrous-$^{13}C^{15}N$ bound (trace F) forms. Traces D and G show the Raman difference spectra between traces B and C and between traces E and F, respectively. (panel B) Verdoheme−Mb complex in the ferrous (trace A), ferrous-$^{12}C^{16}O$-bound (trace B), ferrous-$^{13}C^{18}O$-bound (trace C), ferrous-$^{12}C^{14}N$-bound (trace E), and ferrous-$^{13}C^{15}N$-bound (trace F) forms. Traces D and G show the Raman difference spectra between traces B and C and between traces E and F, respectively. All spectra were obtained using 406.7 nm excitation with ca. 5 mW of laser power except for CO complexes which were obtained with ca. 0.2 mW of excitation laser power.

imidazole-coordinated verdoheme complex shows optical absorption (Figure 6, trace D) as well as resonance Raman

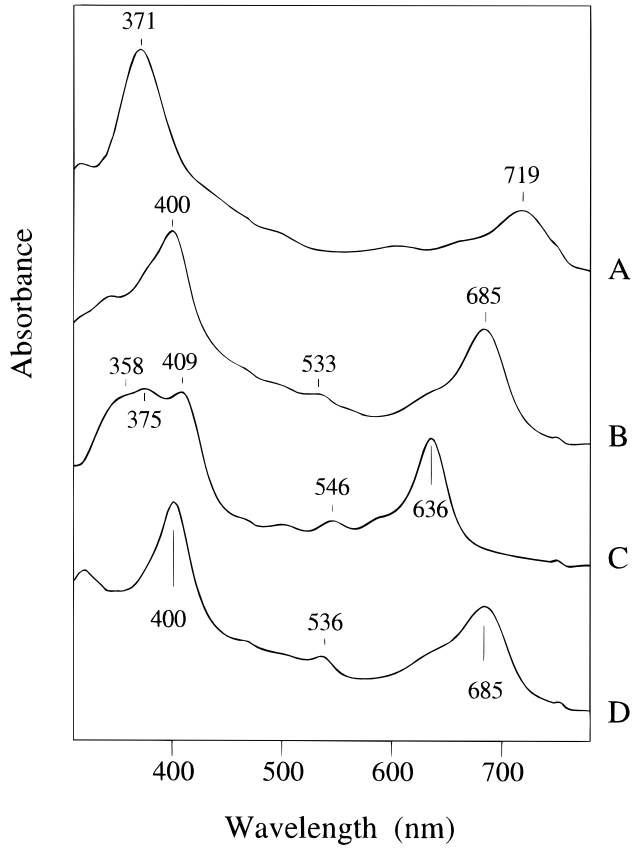

FIGURE 6: Optical absorption spectra of verdoheme model complexes. Bischloride-bound ferric (trace A), monochloride-bound ferrous (trace B), and CO- and chloride-bound ferrous (trace C) forms of protoverdoheme IXα dissolved in CH_2Cl_2. Bisimidazole-bound ferrous protoverdoheme IXa (trace D) dissolved in a 10 M imidazole solution (pH 7). The ordinate scales are arbitrary.

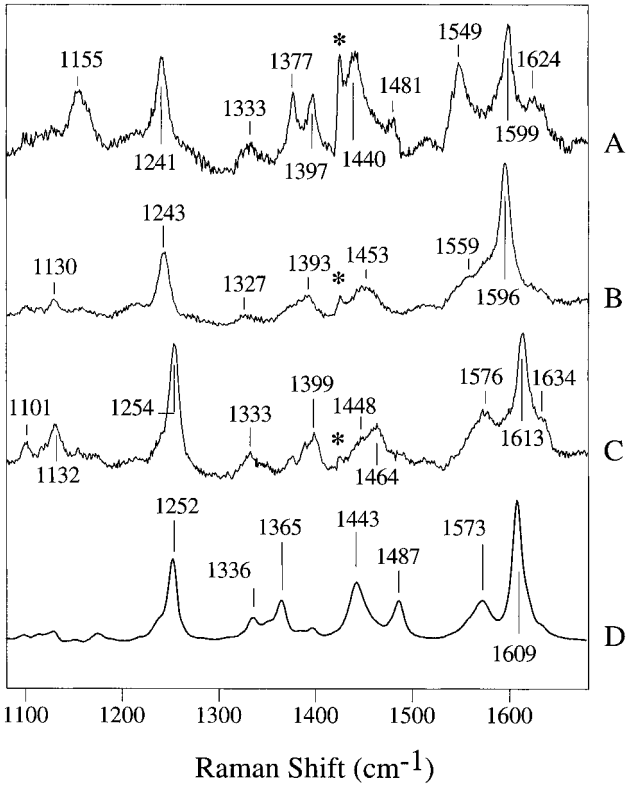

FIGURE 7: Resonance Raman spectra of verdoheme model complexes. Bischloride-bound ferric (trace A), monochloride-bound ferrous (trace B), and CO- and chloride-bound ferrous (trace C) forms of protoverdoheme IXα dissolved in CH_2Cl_2. Bisimidazole-bound ferrous protoverdoheme IXα (trace D) dissolved in a 10 M imidazole solution (pH 7). All spectra were obtained using 406.7 nm excitation with ca. 5 mW of power. Nonresonant solvent Raman lines were removed by subtraction. Asterisks (*) denote the residuals of solvent Raman lines that were removed by subtraction.

(Figure 7, trace D) spectra that are different from those of the CO-bound complex but almost identical with those of the deoxyverdoheme−HO complex (Figure 4, trace A). These results clearly demonstrate that the Raman spectral features of the verdoheme are sensitive to changes in the redox and coordination states as well as in the π-basisity of the axial ligand. In other words, the five-coordinate form of the verdoheme complex shows a Raman spectrum that is distinct from the ferrous six-coordinate complex. It is therefore concluded that the ferrous verdoheme−protein complexes are very likely to be six-coordinate. CO did not photodissociate readily from the CO-bound model complex even with 10 mW of excitation laser power, which forms a clear contrast to the verdoheme−protein complexes that are extremely photolabile.

The optical absorption and resonance Raman spectra for verdoheme dissolved in 10 M imidazole (traces D of Figures 6 and 7), 50% pyridines and 50 mM 2-methylimidazole (0.05% SDS) solutions were qualitatively similar to those of deoxy and CN^--bound protein complexes (data for pyridine and 2-methylimidazole complexes not shown). We could form the CO-bound 2-methylimidazole−verdoheme complex, while pyridine and imidazole complexes do not coordinate with CO. The depolarization ratio measurement of the verdoheme complexed with pyridine showed that all the observed Raman lines are polarized (data not shown).

DISCUSSION

The electronic structures and coordination states of the α-hydroxyheme-HO complexes are described in our previous publication (Mansfield Matera *et al.*, 1996). The ferric complex was shown to be five-coordinate; moreover, the hydroxyl group in the ferric form was shown to be deprotonated, while it is protonated in the ferrous and ferrous-CO-bound forms. The deprotonation gives rise to an oxophlorin resonance structure (Scheme 2, **1**), which we interpreted as the main cause of the atypical Raman spectral pattern observed for the ferric species. The charge neutrality of the prosthetic group likely controls the tautomerism, thus protonating the hydroxy group and yielding a typical porphyrin electronic structure in the ferrous state (Scheme 2, **2**). The ferrous Raman spectra have spectral patterns very similar to those of protoheme compounds, except for the modes such as ν_7 that involve the movement of the α-meso carbon. The Fe-CO and C═O stretching modes appear at frequencies that are similar to the corresponding lines for protoheme compounds. Since the frequencies reflect the amount of π-back donation, the results substantiate the similarity of the electronic states between ferrous α-hydroxyheme and protoheme (Yu & Kerr, 1988; Ray *et al.*, 1994; Wang *et al.*, 1996).

Resonance Raman spectra of the verdoheme complexes show different spectral patterns from those observed for protoheme compounds, but the spectra are similar to those observed for ferric α-hydroxyheme complexes. The polar-

Scheme 2: (Top) Iron Redox-State-Linked Conversion between Ferric Oxophlorin (Structure **1**) and Ferrous Hydroxyheme (Structure **2**) and (Bottom) Two Alternative Verdoheme Structures Derived from Balch *et al*. (1993)

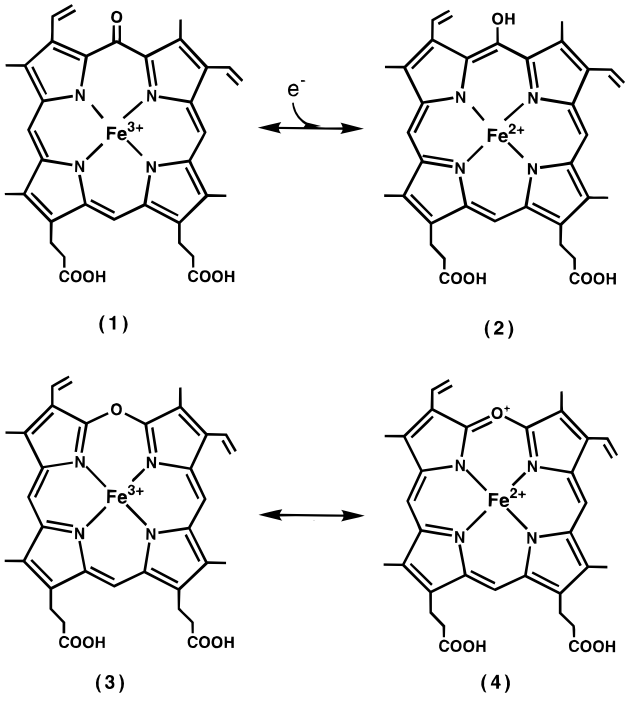

ized Raman lines observed for the bis-pyridine complex of verdoheme show that the verdoheme ring has a symmetry reduced compared with that of protoheme. Two resonance electronic structures have been suggested for verdoheme as depicted in Scheme 2 (Balch *et al.*, 1993). Structure **4** possesses a positive charge on the oxygen atom, while the charge is accommodated on the iron in structure **3**. The reduced symmetry observed for verdoheme, resulting from a disruption of the conjugated π-electron system, suggests a significant contribution from structure **3**. Since the oxophlorin structure **1** assumed for ferric α-hydroxyheme complexes also has an acyclic π-electron-conjugated system, we can infer that the observed similarity of the Raman spectra might be a common property of porphyrins with disruption of the porphyrin π-electron-conjugated systems. An additional example of the disruption is the biliverdin dimethyl ester with a cyclic conformation, whose vibrational structure was analyzed by Smit *et al.* (1993). Consistent with the above arguments, the resonance Raman spectrum of biliverdin has strong overlapped lines between 1580 and 1620 cm^{-1} that are assigned mainly as the pyrrole internal modes. In addition, there are moderate intensity lines at around 1250 cm^{-1} that are assigned to the C−C stretching modes of the vinyl and propionic side chains. Further understanding of the vibrational structure requires analysis of the Raman spectra using isotopically substituted compounds.

The Fe−CO and C═O stretching frequencies of the CO-bound hemes reflect the electronic structure of the heme and its immediate environment (Yu & Kerr, 1988; Ray *et al.*, 1994; Wang *et al*., 1996). The ν_{Fe-CO} lines for verdoheme−protein complexes are located at around 470 cm^{-1}, one of the lowest frequencies known for the Fe−CO stretching mode when a neutral imidazole is the proximal ligand. Fujii (1990) reported the infrared absorption peak for CO-bound verdoheme−Mb complex at 1999 cm^{-1} for $\nu_{C=O}$. Higher

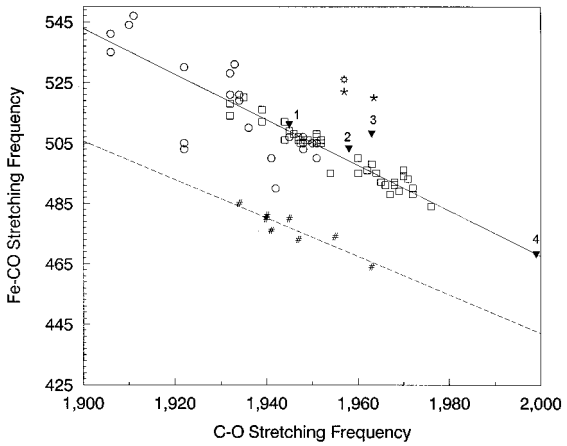

FIGURE 8: Correlation between the Fe−CO and C═O stretching frequencies. The open symbols correspond to a variety of hemoglobins, peroxidases, and model complexes coordinated by imidazole. The #'s correspond to cytochrome P-450s. The starburst corresponds to a porphyrin complexed with tetrahydrofuran, and the asterisks correspond to terminal oxidases. The solid line is a fit to the imidazole-coordinated compounds, and the dashed line is a fit to the thiolate-coordinated compounds. The four numbered points represented by inverted triangles correspond to the following: (1) α-hydroxyheme−Mb, (2) protoheme−HO, (3) α-hydroxyheme−HO, and (4) verdoheme−Mb.

C═O and lower Fe−CO frequencies are attributed to the decreased electron density in the antibonding orbital of CO that is donated from the iron d_π orbital. This agrees with the proposed resonance structure **3** (Scheme 2) that has less electron density on the iron. The correlation plots of the Fe−CO and C═O stretching frequencies are known to be dependent on the trans axial ligand for protoheme compounds (Uno *et al.*, 1987; Yu & Kerr, 1988). Surprisingly, the point for the CO-bound verdoheme−Mb complex as well as that for the α-hydroxyheme−protein complexes all fall on the same line that represents neutral histidine coordination as shown in Figure 8. This result suggests the presence of a neutral histidine as the trans axial ligand for these complexes; however, some care should be taken until further data justify the use of the correlation plot for the hemes other than protoheme.

The CN^- usually binds to ferric heme proteins (Antonini & Brunori, 1971), although several heme proteins, such as peroxidase enzymes, are known to form stable ferrous CN^- complexes as well. Yoshida and Noguchi (1984) reported that CN^- and azide (N_3), another example of a typical ferric ligand, can bind to the ferrous verdoheme−HO complex and inhibit the enzyme turnover. Fujii (1990) estimated the association constants of CN^- and N_3- with verdoheme−Mb that are higher than the corresponding constants for protoheme−Mb in the ferric state. The proposed resonance structure **3** (Scheme 2) with a formal positive charge at the iron bestows many of the characteristics of ferric hemes on ferrous verdohemes, thus explaining its unique ligand binding properties. The observed Fe−CN stretching frequencies of the verdoheme−protein complexes (~470 cm^{-1}) are higher than the reported values for the ferric heme−CN compounds with a linear conformation (435−460 cm^{-1}), suggesting the enhanced donating effect of iron d_π electron density to the CN^- π^* orbital in the ferrous verdoheme (Yu & Kerr, 1988; Boffi *et al.*, 1996). Quantitative understanding of the electronic interaction between CN^- and verdoheme requires careful characterization of the conformation of the Fe−CN

unit using all the isotopomers of CN^- (Al-Mustafa *et al.*, 1994, 1995; Hirota *et al*., 1996) and detection of the C−N stretching mode.

The resonance Raman and optical absorption spectra of the ferrous forms of verdoheme−HO and −Mb complexes are very similar to those of the corresponding CN^--bound complexes, suggesting that the ferrous complexes are six-coordiante. To ascertain the assignment, we have obtained the Raman spectra for the verdoheme compounds with known coordination structures and showed that the ferric six-coordinate, ferrous five-coordinate, and ferrous six-coordinate verdoheme complexes show Raman spectra distinct from each other. We thus conclude that the ferrous state, of the verdoheme−protein complexes are very likely to be six-coordiante. The CO-bound verdoheme model compound does not show photodissociation of CO at 10 mW of excitation laser power, which is in contrast to the HO and apo-Mb complexes that dissociate CO even with 1 mW of excitation. The presence of a sixth axial ligand for the ferrous form of protein complexes can make the rebinding rate of CO slow. Experiments on the CO binding kinetics will be informative in this regard.

The identity of the sixth ligand is unclear. The possibility that the distal histidine (His-64) is the sixth ligand for the Mb complex is excluded, since the optical absorption spectrum of the mutant apoMb with the distal His → Ile replacement reconstituted with verdoheme is identical with that of the wild type complex. The 2-methylimidazole adduct cannot form bis-coordinate heme complexes because of its bulky size; however, a typical six-coordiante spectrum is obtained when 2-methylimidazole is complexed with verdoheme. Since this complex can bind CO, it must have a sixth ligand that can be easily exchanged with CO. We have tentatively assigned hydroxide as the sixth ligand of the verdoheme complexes, although we could not detect any deuterium sensitive lines in the H_2O minus D_2O difference spectrum of the deoxy-HO complex. While the hydroxide is another example of a ligand which binds to a ferric iron, the negative charge of the hydroxide might explain the spectral similarities between ferrous and CN^--bound forms.

Conclusions. The ferric forms of α-hydroxyheme complexes of HO and apo-Mb have disrupted π-electron-conjugated systems, while the electronic structures of ferrous and ferrous-CO-bound forms are similar to those of the protoheme compounds. The α-hydroxy group is deprotonated in the ferric state, while it is protonated in the ferrous state. Thus, the ionization of the group controls the electronic structure of the α-hydroxyheme. The ferrous verdoheme−protein complexes have a Raman spectral pattern that is similar to that of the ferric α-hydroxyheme complexes, which is also interpreted as the result of a disrupted π-electron-conjugated pathway in the heme macrocycle. A resonance structure with a positive charge on the iron is assumed to have a significant contribution.

Both ferric and ferrous forms of the α-hydroxyheme protein complexes are five-coordinate with presumably a neutral histidine as the proximal ligand. The ferrous verdoheme−protein complexes are six-coordinated. A neutral histidine and a hydroxide ion are assumed to be the proximal and distal ligands, respectively.

The peculiar ligand binding properties of α-hydroxyheme and verdoheme are interpreted as the result of the intrinsic properties of each of the heme derivatives. The α-hydroxyheme has an ionizable group that is dependent on the iron redox state. The verdoheme has a positive charge that governs its electronic character. Thus, the electronic properties of the intermediates in the heme oxygenase mechanism can be inferred from the resonance Raman spectra of these model complexes. Unique properties of these complexes illustrate the importance of studying them in order to clarify the molecular mechanism of the degradation of the corresponding intermediates in heme oxygenase.

ACKNOWLEDGMENT

We thank Dr. Yi Dou for the mutant Mb and Dr. Catharina T. Migita for her comments. S.T. gratefully acknowledges Drs. Yoshitsugu Shiro and Tetsutaro Iizuka for their encouragement.

REFERENCES

Abe, M., Kitagawa, T., & Kyogoku, Y. (1978) *J. Chem. Phys. 69*, 4526−4534.
Al-Mustafa, J., & Kincaid, J. R. (1994) *Biochemistry 33*, 2191−2197.
Al-Mustafa, J., Sykora, M., & Kincaid, J. R. (1995) *J. Biol. Chem. 270*, 10449−10460.
Antonini, E., & Brunori, M. (1971) in *Hemoglobins and Myoglobins in Their Reactions with Ligands*, Elsevier, Amsterdam.
Balch, A. L., Latos-Grazynski, L., Noll, B. C., Olmstead, M. M., Szterenberg, L., & Safari, N. (1993) *J. Am. Chem. Soc. 115*, 1422−1429.
Boffi, A., Takahashi, S., Rousseau, D. L., & Chiancone, E. (1996) *Biochemistry* (submitted for publication).
Brown, S. B., & King, R. F. G. J. (1976) *Biochem. Soc. Trans. 4*, 197−201.
Chang, C. K., Aviles, G., & Bag, N. (1994) *J. Am. Chem. Soc. 116*, 12127−12128.
Dawson, J. H. (1988) *Science 240*, 433−439.
Fujii, H. (1990) Studies on the Electronic Structure and Reactivities of Catalytic Intermediates in Heme Enzymes, Ph.D. Thesis, Kyoto University, Kyoto, Japan.
Henry, E. R., Rousseau, D. L. Hopfield, J. J., Noble, R. W., & Simon, S. R. (1985) *Biochemistry 24*, 5907−5918.
Hernandez, G., Wilks, A., Paolesse, R., Smith, K. M., Ortiz de Montellano, P. R., & La Mar, G. N. (1994) *Biochemistry 33*, 6631−6641.
Hirota, S., Ogura, T., Shinzawa-Itoh, K., Yoshikawa, S., & Kitagawa, T. (1996) *J. Phys. Chem. 100*, 15274−15279.
Hu, S., & Spiro, T. G. (1993) *Biophys. J. 64*, A157.
Ishikawa, K., Sato, M., & Yoshida, T. (1991) *Eur. J. Biochem. 202*, 161−165.
Ito-Maki, M., Ishikawa, K., Matera, K. M., Sato, M., Ikeda-Saito, M., & Yoshida, T. (1995) *Arch. Biochem. Biophys. 317*, 253−258.
Kikuchi, G., & Yoshida, T. (1983) *Mol. Cell. Biochem. 53/54*, 163−183.
Kitagawa, T. (1988) in *Biological Applications of Raman Spectroscopy* (Spiro, T. G., Ed.) Vol. 3, pp 97−131, Wiley, New York.
Maines, M. D. (1988) *FASEB J. 2*, 2557−2568.
Mansfield Matera, K., Takahashi, S., Fujii, H., Zhou, H., Ishikawa, K., Yoshimura, T., Rousseau, D. L., Yoshida, T., & Ikeda-Saito, M. (1996) *J. Biol. Chem. 271*, 6618−6624.
Morishima, I., Fujii, H., Shiro, Y., & Sano, S. (1986) *J. Am. Chem. Soc. 108*, 3858−3860.
Morishima, I., Fujii, H., Shiro, Y., & Sano, S. (1995) *Inorg. Chem. 34*, 1528−1535.
Noguchi, M., Yoshida, T., & Kikuchi, G. (1981) *J. Biochem. 90*, 1671−1675.
Noguchi, M., Yoshida, T., & Kikuchi, G. (1983) *J. Biochem. 93*, 1027−1036.
Poulos, T. L. (1988) *Adv. Inorg. Chem. 7*, 1−36.
Ray, G. B., Li, X.-Y., Ibers, J. A., Sessler, J. L., & Spiro, T. G. (1994) *J. Am. Chem. Soc. 116*, 162−176.

Saito, S., & Itano, H. A. (1982) *Proc. Natl. Acad. Sci. U.S.A. 79*, 1393−1397.
Saito, S., & Itano, H. A. (1986) *J. Chem. Soc., Perkin Trans.*, 1−7.
Sano, S., Sano, T., Morishima, I., Shiro, Y., & Maeda, Y. (1986) *Proc. Natl. Acad. Sci. U.S.A. 83*, 531−535.
Smit, K., Matysik, J., Hildebrandt, P., & Mark, F. (1993) *J. Phys. Chem. 97*, 11887−11900.
Spiro, T. G., & Li, X.-Y. (1988) in *Biological Applications of Raman Spectroscopy* (Spiro, T. G., Ed.) Vol. 3, pp 1−37, Wiley, New York.
Stevens, C. F., & Wang, Y. (1993) *Nature 364*, 147−149.
Suematsu, M., Goda, N., Sano, T., Kashiwagi, S., Egawa, T., Shinoda, Y., & Ishimura, Y. (1995) *J. Clin. Invest. 96*, 2431−2437.
Sun, J., Loehr, T. M., Wilks, A., & Ortiz de Montellano, P. R. (1994) *Biochemistry 33*, 13734−13740.
Takahashi, S., Wang, J., Rousseau, D. L., Ishikawa, K., Yoshida, T., Host, J. R., & Ikeda-Saito, M. (1994a) *J. Biol. Chem. 269*, 1010−1014.
Takahashi, S., Wang, J., Rousseau, D. L., Ishikawa, K., Yoshida, T., Takeuchi, N., & Ikeda-Saito, M. (1994b) *Biochemistry 33*, 5531−5538.
Takahashi, S., Ishikawa, K., Takeuchi, N., Ikeda-Saito, M., Yoshida, T., & Rousseau, D. L. (1995) *J. Am. Chem. Soc. 117*, 6002−6006.
Teale, F. W. J. (1959) *Biochim. Biophys. Acta 35*, 543.
Tenhunen, R., Marver, H. S., & Schmid, R. (1969) *J. Biol. Chem. 244*, 6388−6394.
Uno, T., Nishinura, Y., Tsuboi, M., Makino, R., Iizuka, T., & Ishimura, Y. (1987) *J. Biol. Chem. 262*, 4549−4556.
Verma, A., Hirsch, D. J., Glatt, C. E., Ronnett, G. V., & Snyder, S. H. (1993) *Science 259*, 381−384.
Wang, J., Caughey, W. S., & Rousseau, D. L. (1996) in *Methods in Nitric Oxide Research* (Freelisch, M., & Stamler, J., Eds.) Wiley, New York (in press).
Wilks, A., & Ortiz de Montellano, P. R. (1993) *J. Biol. Chem. 263*, 22357−22362.
Yoshida, T., & Kikuchi, G. (1978a) *J. Biol. Chem. 253*, 4224−4229.
Yoshida, T., & Kikuchi, G. (1978b) *J. Biol. Chem. 253*, 4230−4236.
Yoshida, T., Noguchi, M., & Kikuchi, G. (1980a) *J. Biol. Chem. 255*, 4418−4420.
Yoshida, T., Noguchi, M., & Kikuchi, G. (1980b) *J. Biochem. 88*, 557−563.
Yoshida, T., Noguchi, M., Kikuchi, G., & Sano, S. (1981) *J. Biochem. 90*, 125−131.
Yoshida, Y., & Noguchi, M. (1984) *J. Biochem. 96*, 563−570.
Yoshida, Y., Noguchi, M., & Kikuchi, G. (1982) *J. Biol. Chem. 257*, 9345−9348.
Yu, N.-T., & Kerr, E. A. (1988) in *Biological Applications of Raman Spectroscopy* (Spiro, T. G., Ed.) Vol. 3, pp 39−95, Wiley, New York.
Zhuo, M., Small, S., Kandel, E. R., & Hawkins, R. D. (1993) *Science 260*, 1946−1950.

BI962361Q